Chromium removal from aqueous solutions using new silica gel conjugates of desferrioxamine or diethylenetriaminepentaacetic acid

Aamir Rasheed[1] · Alexandrina Aparecida Costa Carvalho[2] · Gabriel Gustinelli Arantes de Carvalho[2] · Tahseen Ghous[3] ·
Cassiana Seimi Nomura[2] · Breno Pannia Esposito[2]

Abstract

Desferrioxamine (DFO) and diethylenetriaminepentaacetic acid (DTPA) conjugated with silica gel (IDFOSG and IDTPASG, respectively) were evaluated as adsorbents for chromium in aqueous solutions. Different parameters affecting adsorption such as pH, sorbent dosage, contact time, sample volume and potential of interfering ions have been optimized. The optimum pH for chromium binding was 4 for 100 mg of adsorbents at 5 min of table shaking with 5 mL sample volume of chromium solutions. Langmuir adsorption model described the removal of chromium ions. The adsorption capacity for chromium was 90% for IDFOSG and 83% for IDTPASG in single solutions, and at least 75% in multielemental solutions. Considering the removal efficacy, regeneration and stability, DFO-grafted silica gel was generally superior to its DTPA counterpart and may be applied to the removal of traces of chromium species from natural waters.

Keywords Chromium · Surface functionalization · Silica gel · Desferrioxamine · Diethylenetriaminepentaacetic acid

Introduction

Metallurgical, chemical and refractories industries discharge wastewater containing chromium (Cr) into the environment (Lyu et al. 2017, Miretzky & Cirelli 2010, Yang & Lee 2006), under its trivalent or hexavalent forms, bringing about severe biological and ecological damages (Kotaś & Stasicka 2000, Lyu et al. 2017). The toxicity of Cr(III) for fishes is reported at concentrations higher than 5.0 mg/L in water (Sari et al. 2008), while serious health concerns for human

are associated with Cr(VI), a known carcinogenic for plants and animals (Miretzky & Cirelli 2010, Qiu et al. 2009). Also, reduced microbial growth is observed in the presence of Cr(VI) (Karthik et al. 2017, Wani et al. 2018), which affects soil fertility and decreases crop productivity (Dutton & Fisher 2011, Oves et al. 2013, Takahashi et al. 2012). In aqueous media, Cr(VI) is more soluble and mobile than Cr(III) (Dong et al. 2017). In order to preserve environment and eco-systems quality, Cr(VI) removal from aqueous media is crucial.

Electrochemical processes, ion exchange, membrane filtration, reverse osmosis, flotation and chemical precipitation are different methods employed for the removal of toxic metal ions. For the removal of Cr(VI) in dilute solutions, these methods are either expensive or troublesome. However, adsorption processes are economical, efficient, flexible and reversible; therefore, they are proving significant for chromium removal from wastewater (Kandile & Nasr 2014, Li et al. 2016, Sethy & Sahoo 2019, Sugumaran & Karim 2017).

The adsorption of numerous metal ions from wastes by chelating resins is well studied. An enhanced preconcentration factor at extensive pH ranges is observed when chelating agents are adsorbed onto a solid adsorbent (Jal et al. 2001). On the silica gel (SG) surface, silanol groups (Si–OH) are distributed throughout, providing an opportunity for ligand

✉ Breno Pannia Esposito
breno@iq.usp.br

1 Department of Chemistry, University of Azad Jammu and Kashmir, Muzaffarabad, Azad Kashmir 13100, Pakistan

2 Department of Fundamental Chemistry, University of São Paulo, Av. Prof. Lineu Prestes, 748, São Paulo, SP 05508-000, Brazil

3 Department of Chemistry, Mirpur University of Science & Technology (MUST), Mirpur, Azad Jammu and Kashmir 10250, Pakistan

immobilization by chemical modification of its surface (Dey et al. 2006, Liang & Chen 2005). The stability, immobility, insolubility and high efficiency are key advantages of the covalent grafting of chelating molecules on silica surface (Jal et al. 2001).

Desferrioxamine B (DFO) belongs to the hydroxamate family of siderophores (Powell et al. 1980). It is remarkably avid for trivalent iron, finding its chief role in the treatment of iron overload disorders like thalassaemia, and aluminium poisoning (Aaseth et al. 2015). Many attempts were made to immobilize DFO on multiple supports to develop methods for the treatment of metals overload, biosensing or metal speciation (Alberti et al. 2014, Alberti et al. 2015, Su et al. 2011, Takagai et al. 2007, Wenk et al. 2001). Chelation therapy by another chelator, diethylenetriaminepentaacetic acid (DTPA), has also been extensively studied as a method for removing elements from the body (Parker et al. 1962, Slobodien et al. 1973). DTPA-modified silica gel and chitosan were reported for adsorption of certain metals including Cr(VI) (Bhatt et al. 2015, Repo et al. 2011). DFO immobilized in mesocellular silica foams for chelation of divalent and trivalent metal ions was reported (Schwabe et al. 2018). The stability, immobility, insolubility and high efficiency are key advantages of the covalent grafting of chelating molecules on silica surface (Jal et al. 2001).

In the present work, for the first time, DFO and DTPA were grafted on activated silica gel forming silica gel conjugates (SGC) IDFOSG and IDTPASG, respectively. The optimization of adsorption conditions for chromium species is described, along with their performances in multielemental solutions.

Materials and methods

Chemicals

Silica gel, Chelex 100® sodium form, hepes, ferrous ammonium sulphate and acetic acid were from Sigma-Aldrich. Diethylenetriamine pentaacetic acid was from Acros. Aminopropyltriethoxysilane (APTES) and hydrochloric acid were from Fluka. Sodium phosphate dibasic and potassium chloride were from Cromoline (Brazil). Sodium phosphate monobasic was from Reagen (Brazil). Potassium hydrogen phthalate, monopotassium phosphate, sodium hydroxide, nitric acid, acetone, toluene, ethyl alcohol, pyridine, acetic anhydride and sodium chloride were from Synth (Brazil). Calcein and sulphuric acid were from Vetec (Brazil). Glutaraldehyde was from Nuclear (Brazil). Desferrioxamine mesylate salt (Cristália, Brazil) was a gift from Associação Brasileira de Talassemia (ABRASTA). Cr(VI) atomic absorption standard was from SpecSol, and Na(I), Mn(II), Cu(II), Zn(II), Ba(II), Al(III), Fe(III) and Cr(III) standards containing

1000 mg L^{-1} were from Tritisol. Sodium carbonate was from Fisher Chemicals. The reagents were at least 99% pure and used without further purification. Ultrapure water obtained from a Milli-Q purification system (Millipore) or a OS10LXE reverse osmosis (Gehaka, Brazil) was used throughout the studies. Potassium phthalate buffer was prepared with 0.1 M potassium hydrogen phthalate and pH adjusted to 4. Sodium carbonate buffer was prepared with 0.1 M sodium carbonate, and pH adjusted to 10. Hepes buffered saline (HBS) was hepes 20 mM and NaCl 150 mM, washed with Chelex®100 (1 g/ 100 mL) with pH adjusted to 7 and 7.4.

Instruments

Cr determination in aqueous solutions was performed in a Vario 6 flame atomic absorption spectrometer (Analytik Jena, Germany). Instrument parameters employed include hollow cathode lamp of chromium with 357.9 nm wavelength, 5 mA applied current, 0.8 nm spectral band-pass and deuterium background correction, air flow of 400 L h^{-1}, acetylene flow of 80 L h^{-1}, as recommended by manufacturer. The analytical solutions containing SGC were mixed by using a shaker table (Quimis, Brazil). Bench centrifuges (Q222TM, Quimis and Eppendorf AG 22331) were used to separate the supernatant and SGC solids. All pH measurements were made using a digital pH meter (Gehaka PG1800), and mixing was made by using vortex mixer (Vixer Korea). An analytical balance (AUX220, Shimadzu) was used for weighing purposes.

Surface grafting of DFO and DTPA on SG

The schematics of the grafting are shown in Fig. 1. High-purity silica gel (SG), pore size 60 Å and 230–400 mesh size, was refluxed in 6 M HCl for 3 h. After an extensive washing with ultrapure water, a conventional furnace (EDG10P-S) was used for drying SG at 200 °C for 24 h. The aminopropylation of SG was carried out by adding 15 mL of 3-aminopropyltriethoxy silane (APTES) to 25 g of SG in 150 mL of toluene. Magnetic stirring at 200 rpm was maintained for 16 h. The reaction mixture was filtered to get aminopropyl silica gel (APSG). Several rounds of washing of APSG with toluene and acetone (100 mL each) were conducted before drying in oven at 65 °C for 24 h (Repo et al. 2009).

The surface grafting of DFO on SG was carried out by adding 2 g of APSG to a 2.5% glutaraldehyde solution (final concentration) in 25 mL of 0.1 M sodium phosphate buffer at pH 7. The reaction mixture was kept under continuous stirring for 2 h at room temperature. The product was filtered and washed with 250 mL of water and dried again at 65 °C for 24 h, producing activated APSG. One gram of DFO was mixed with 2 g of activated APSG in 10 mL of water (Ljunggren et al. 1992). The mixture was allowed to react
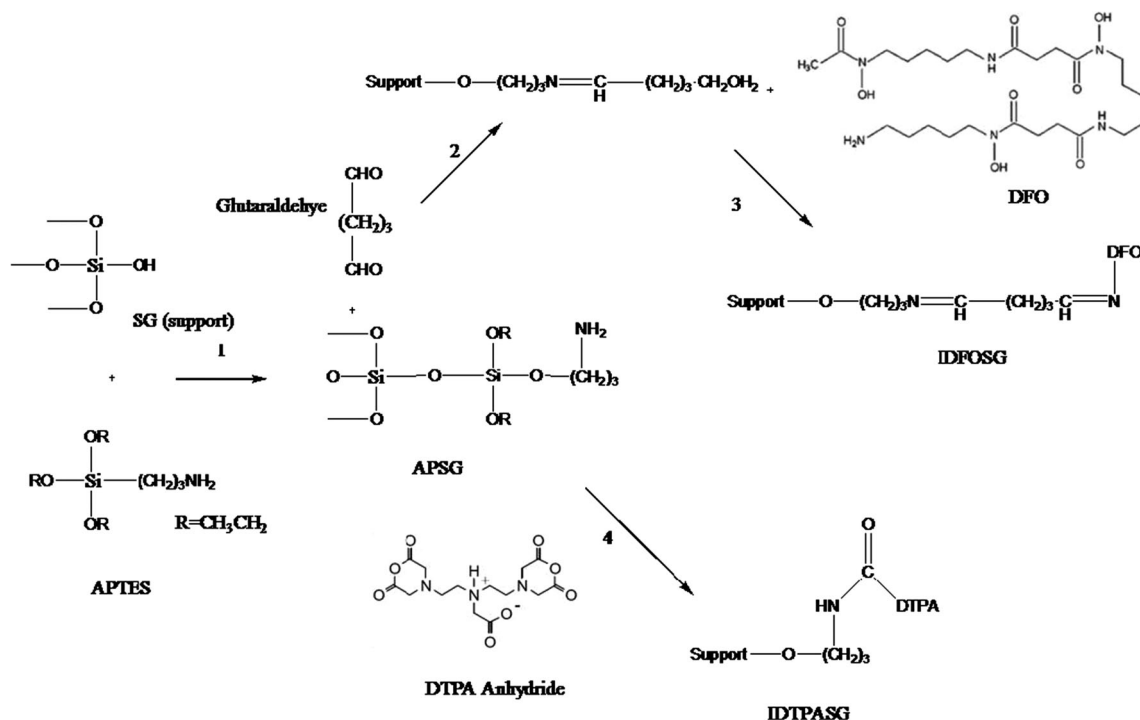
Fig. 1 Scheme for the surface functionalization of DFO and DTPA on SG

for 4 h, and then filtered and washed with 100 mL of water. Surface grafted immobilized DFO on SG (IDFOSG) was dried at 65 °C for 24 h and kept in an airtight polypropylene vial.

DTPA anhydride was prepared by a modified version of the protocol by Tülü et al. (Tülü & Geckeler 1999). Ten grams of DTPA (25 mmol) were suspended in 20 mL of pyridine with subsequent addition of 20 mL of acetic anhydride and refluxed at 65 °C for 24 h. The product was filtered, washed with 25 mL of acetic anhydride and 25 mL of diethyl ether and dried in oven at 65 °C for 24 h. Three grams of APSG and 8 g of DTPA anhydride were added and 100 mL of 1:1 ethanol and acetic acid solution was prepared. A yellowish product formed, indicating the completion of reaction and 4 M NH$_4$OH, 1:1 mixture of ethanol/acetic acid, water and methanol were used for extensive washing after filtration (Hughes & Rosenberg 2007). Surface grafted immobilized DTPA on SG (IDTPASG) was dried at 65 °C for 24 h and kept in an airtight polypropylene vial.

Estimation of DFO and DTPA load on SGC by competition studies with calcein

Upon coordination to iron, the fluorescence of calcein is stoichiometrically quenched and may be regenerated after treatment with other high affinity chelators such as DFO and DTPA (Baccan et al. 2012). Therefore, fluorescence recovery of a known solution of calcein-iron (CAFe), after treatment with IDFOSG or IDTPASG, is a quick method to quantify the

amount of immobilized chelator. For this, calcein and ammonium ferrous sulphate in equimolar quantities were used to prepare 5 mM stock solutions of CAFe in HBS/Chelex. All the other CAFe solutions were also prepared in HBS/Chelex. In 1.5 mL vials, weighed amounts of SGC were transferred and treated with 1 mL of 100 μM CAFe. Free chelators DFO and DTPA at 100 μM were used as controls. The suspensions were vortexed for 2 min and centrifuged for 5 min at 4000 rpm at room temperature. Samples of the supernatants (100 μL) were then transferred to clear, flat bottom 96 well microplates, and their fluorescence was registered with a BMG FluoStar Optima instrument ($\lambda_{exc}/\lambda_{em} = 485/520$ nm).

Sorption optimization

In order to evaluate the effect of SGC on Cr uptake from aqueous solutions, it was conducted optimizations of different parameters: pH, SGC mass, shaking (contact) time and sample volume. The experiments were conducted in 15 mL polypropylene conical centrifuge tubes. Agitation was carried out by a Quimis table shaker. Centrifugation was performed in a Quimis Q222TM at 2790 rcf for 5 min at room temperature. The amount of Cr in the supernatants was quantified by atomic absorption flame spectroscopy. Uptake ($\alpha\%$) is defined as:

$$\alpha(\%) = \left(\frac{c_i - c_e}{c_i}\right) \times 100 \qquad (1)$$

where c_i and c_e are the initial and equilibrium concentrations of chromium, respectively (Carvalho et al. 2019).

- pH optimization: Hydrochloric acid in potassium chloride was used for adjusting the pH to 2. Buffers of pH 4, 7 and 10 were made from potassium hydrogen phthalate, potassium phosphate and sodium carbonate, respectively. Volume of 3 mL of Cr solution (1 mg L^{-1}) in these buffers were mixed with 50 mg of SGC.
- SGC mass optimization: The effect of different masses of SGC (6.25–200 mg) on the uptake degree of 3 mL of 1 mgL^{-1} of Cr(VI) at pH 4 was studied.
- Contact time optimization: The mixtures of 1 mg L^{-1} Cr(VI) (pH 4) and 100 mg of SGC were shaken for 5–1440 min.
- Sample volume optimization: Samples (1–10 mL) of 1 mg L^{-1} of Cr(VI) at pH 4 reacted with 100 mg of SGC for 5 min.

Langmuir isotherms

Adsorption isotherms were determined in the range 0.5–2000 mg L^{-1} of Cr(VI) solutions treated with 100 mg of SGC in a 5 mL sample volume. Data were fitted with the function LangmuirEXT1 (Origin® 2016; OriginLab Corporation).

Effect of potentially interfering ions

The effect of various interfering ions on Cr(VI) sorption was analyzed in 5 mL of 1 mg L^{-1} of Cr(VI) solution at pH 4, by adding different amounts of Na(I), Mn(II), Cu(II), Zn(II), Ba(II), Al(III) and Fe(III) according to the ratios listed in Table S1. From the Ordinance 2914/2011 of the Brazilian Ministry of Health, the permissible limits of these ions and Cr(VI) were taken to measure the ratio X/Cr(VI) where X is the interfering ion (Brazil 2011).

The calibration curve for Cr(VI) at pH 4 was built from 0.25 to 2.5 mg L^{-1}. The limit of detection (LOD) was estimated by $(3 \times SD)/a$, where SD is the standard deviation of 10 measurements of absorbance of blank solution containing buffered media (pH 4), and a is the calibration curve slope. The limit of quantification (LOQ) was defined as $(10 \times SD)/a$ (Currie 1995).

Regeneration studies

The stability and regeneration were assessed by desorption experiments (Bhatt et al. 2015). For this, 400 mg of IDFOSG or IDTPASG were preloaded with 4 mg L^{-1} Cr(VI) at pH 4 in 20 mL sample volume. After filtering and washing with ultrapure water, 100 mg of the dry Cr-loaded IDFOGC were added to 5 mL of 0.1 M NaOH, H$_2$SO$_4$, HCl and HNO$_3$ separately. After 5 min of table shaking and centrifugation, an aliquot of the supernatant was removed for the quantification of Cr and determination of the % desorption, defined as:

$$\%desorption = \left(\frac{Cr \text{ in supernatant after desorption}}{Cr \text{ in the supernatant after sorption onto SGC}} \right) \times 100 \qquad (2)$$

(Kumar & Rajesh 2013). The usability of SGC was tested by three successive sorption–desorption cycles.

Results and discussion

Chemical characterization of IDFOSG and IDTPASG

FTIR spectra are illustrated in Fig. 2 according to sequence of reactions for grafting of DFO and DTPA on SG. In SG and in its conjugates, the band around 1634, 1048, 970 and 795 cm^{-1} are assigned to Si–O–Si bond stretching vibrations which are related with condensed silica network (Bertoluzza et al. 1982, Jitianu et al. 2002, Li et al. 2008). The broad IR absorption band from 3500 to 3055 cm^{-1} is due to superimposed stretching modes of Si-OH groups and the hydroxyl groups of adsorbed water (Najafi et al. 2012).

The decrease in intensity of peaks between 3400 and 3100 and 970 and 1634 cm^{-1} and appearance of a less intense N–H bending vibration around 697 cm^{-1}, which can be found in samples of APSG, confirm the incorporation of small amount of amino groups on silica gel surface (Li et al. 2008). The appearance of absorbance peaks around 1000–1200 cm^{-1} is due to C-N stretching vibrations (Shriner et al. 1948). However, its determination is made difficult by overlapping Si-O-Si stretches at 1000–1130 cm^{-1} and Si-CH$_2$-R stretches at 1200–1250 cm^{-1} (Maria Chong & Zhao 2003, White & Tripp 2000). The absorption band at 1635 cm^{-1} in SG is shifted to 1560 cm^{-1} in APSG probably due to N-H vibrations.

DFO exhibits the same spectral hallmarks as previously described (Siebner-Freibach et al. 2005, Umemura et al. 2017). The bands at 2875 and 2929 cm^{-1} are due to stretching vibrations of the CH$_2$ backbone of DFO. The vibrations typical of the hydroxamic group appear at 1619 cm^{-1} and are related to stretching vibrations of C=O. For the primary amine, two N–H stretches appear at 3098 and 3307 cm^{-1}. The peak at 1160 cm^{-1} may be due to C-O or C-C stretching. The bands at 1459, 1160 and 1014 cm^{-1} are due to N-H, C-C bending vibrations and N-O stretching vibrations of the hydroxamate group, respectively. The appearance of peaks at 2929, 3308, 1623, 1566, 1459 and 1044 cm^{-1} in IDFOSG which were originally absent in SG and APSG and the retention of peaks due to Si-O-Si stretch vibration modes of the silica gel show the conjugation of DFO to the surface of
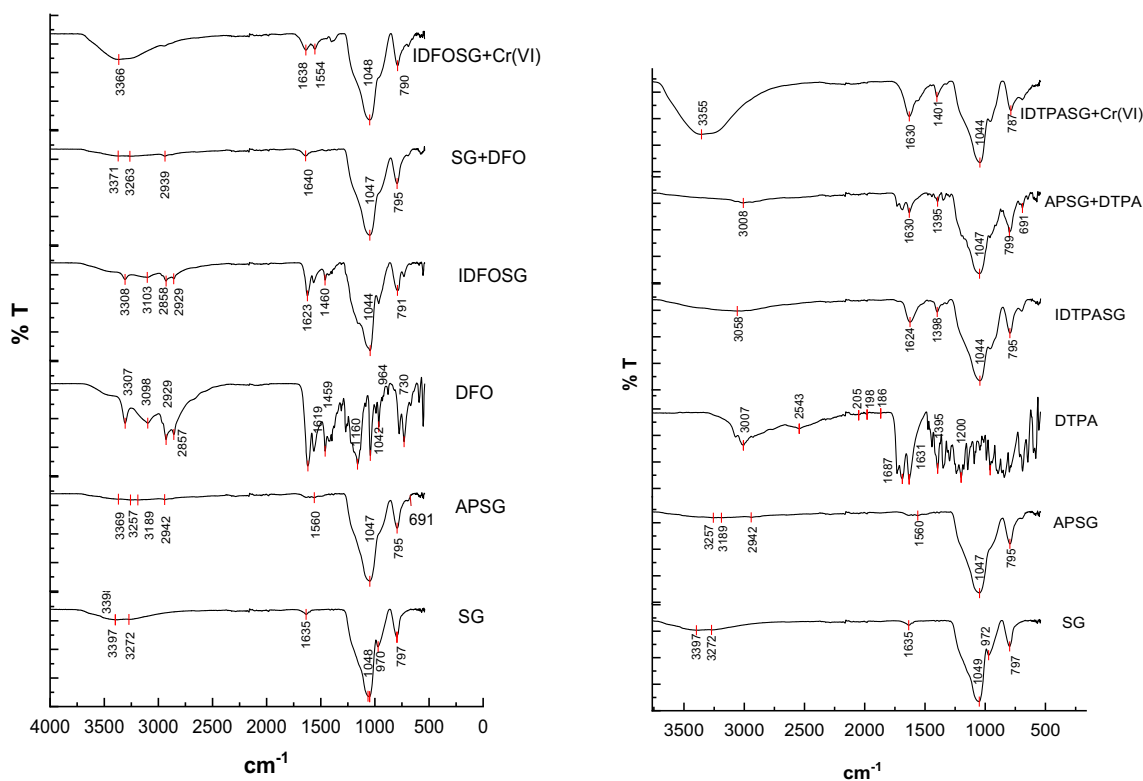
Fig. 2 FTIR spectra of the intermediates involved in grafting DFO or DTPA on SG

APSG. The decrease in signal intensity at 3307 cm^{-1} and the appearance of a relatively intense signal at 1623 cm^{-1} indicate the formation of the Schiff's base involving the amino group and the aldehyde group via glutaraldehyde cross-linking between DFO and APSG (Beppu et al. 2007). The absorption of the amide of Schiff's base is probably overlapping the amide band of DFO. The mixture containing DFO and SG has peaks at 1047, 795, 1640, 2939 and 3371 cm^{-1} which are mostly related to SG IR spectrum.

The spectrum of chromium-loaded IDFOSG showed a peak for at 691 cm^{-1} (Supplementary Fig. S1) attributed to the Cr–O stretch (Bhatt et al. 2015) showing interaction of hydrogen chromate (HCrO$_4^-$, the main Cr(VI) species at pH 4 (Michael Sperling 1992, Wu et al. 2009)) with the surface grafted DFO molecule (Fig. S1). On comparing with the metal-loaded sample, it is observed that there is a shift in wave number of dominant peaks due to hydroxamate group binding to Cr(VI) or its adsorption on the surface of IDFOSG. After Cr(VI) loading, a peak at 1460 cm^{-1} in IDFOSG was displaced to 1554 cm^{-1}, and low intensity narrow peaks at 2929, 2858, 3103 and 3308 cm^{-1} converged into a broad intense peak around 3366 cm^{-1} probably due to either to H–O–H stretching vibration bands of adsorbed water molecules, or to the presence of hydrogen chromate (HCrO$_4^-$).

ITDPASG was similarly characterized (Fig. 2). Free DTPA exhibits reported carboxylic acid O–H stretch at 3007 cm^{-1} and bands at 1687 and 1631 cm^{-1}, corresponding to the C = O

bending in −COOH. An appearance of an amide C = O stretch at 1624 cm^{-1} in IDTPASG which is originally absent in APSG shows the formation of amide bond between APSG and DTPA. Beppu et al. (Beppu et al. 2007) reported that this type of linkage showed absorption at 1655 cm^{-1}. The IR spectrum of chromium-loaded IDTPASG showed the same pattern of shifting of wave number of dominant peaks associated with IDFOSG.

Estimation of DFO and DTPA load on SG by competition studies with calcein

The extent of surface functionalization of SG with DFO and DTPA was assessed by the regeneration of calcein fluorescence from ferric calcein, CAFe (Fig. 3). The quenching of calcein fluorescence by iron is stoichiometrical and reversible upon reaction with chelators with higher affinity for iron (e.g., DFO and DTPA); therefore, fluorescence emission from CAFe interacting with SGC can be used to quantify the chelator load of SGC. Initially, as a proof of concept, it was verified that a 100-mg sample of either IDFOSG or IDTPASG (but not untreated SG) was able to regenerate calcein fluorescence (Supplementary Fig. S2), indicating that the binding properties of DFO and DTPA were not affected after conjugation. Then, the dose-dependent relation between regeneration of fluorescence and concentration of conjugated molecules was found to be linear in the range of 1.56 to 50 mg

Fig. 3 **a** Fluorescence recovery of CAFe upon iron sequestration by IDFOSG and IDTPASG. **b** Chelator load of SGC. a.u.: arbitrary fluorescence units
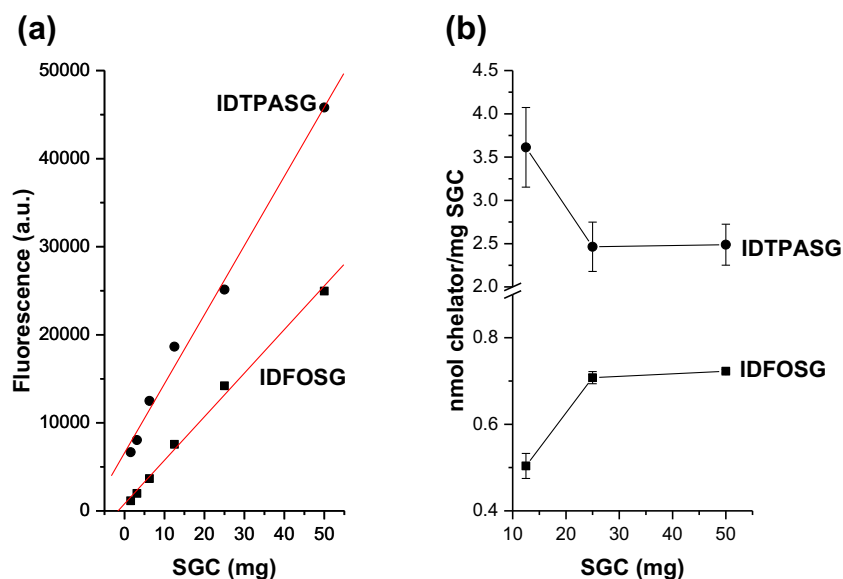
for IDFOSG and IDTPASG (Fig. 3a). The molar amounts of DFO and DTPA per mass unit of SG were calculated using calibration curves relating chelator concentration to fluorescence increase (Supplementary Fig. S3), followed by normalization to the mass of SGC (Fig. 3b). The average DFO and DTPA load in SG was 0.611 ± 0.011 and 3.05 ± 0.43 nmol mg^{-1}, respectively. The DTPA load was greater than DFO per mass unit of SG as the initial reaction conditions were slightly different, with higher chelator/APSG ratio used in the synthesis of IDTPASG.

Sorption optimization

The influence of pH on Cr(VI) and Cr(III) uptake by SGC is shown in Fig. 4 a. The complexation of several metal ions with DFO has been reported (Alta et al. 2014, Darr et al. 1987, Domingo 2006, Duckworth & Sposito 2005, Gabizon et al. 1988, Randal J. Keller 1991); however, the complexation of Cr(VI) is less frequently discussed (Christoffersen et al. 1987, Ke Jian Liu 1997, Xianglin Shi 1992). At pH < 7, the coordination sites of both IDTPASG and IDFOSG are protonated; therefore, Cr(III) is excluded from binding. This changes in neutral-alkaline pH, because of ligand deprotonation; however, Cr(III) also precipitates as oxides or hydroxides at pH > 7 (Rai et al. 1987). At pH 2–4, Cr(VI) exists mainly (66%) as $HCrO_4^-$ and also (34%) as $Cr_2O_7^{2-}$. These proportions shift to mainly CrO_4^{2-} at pH 10. Since maximum Cr(VI) binding was found at acidic pH when most binding sites are protonated and therefore without charge, it is probable that deprotonation (with increase in the negative charge of the SGC) will not favour the binding of the highly negative CrO_4^{2-} ion.

Therefore, Cr(VI) and pH = 4 were selected for further studies because at this condition, the uptake degree of

hexavalent chromium by IDFOSG was ~88% and ~75% for IDTPASG.

The effect of different masses of IDFOSG and DTPASG on the uptake degree of Cr(VI) (3 mL; 1 mg L^{-1}; pH 4) was investigated to optimize its value. It was observed that up to 100 mg of SGC, the uptake of Cr(VI) increases, reflecting the increase of interactive sites for Cr(VI) on the surface and then levelling off (Fig. 4b). Less than 10% Cr(VI) uptake was observed for the reference material (SG). Hence, a mass of 100 mg was selected for further studies.

The effect of contact time is an important parameter to optimize adsorbent performances. The interaction of Cr(VI) (3 mL; 1 mg L^{-1}; pH 4) with 100 mg of SGC up to 1440 min of table shaking was determined (Fig. 4c). Two trends were observed. Firstly, no marked change in behaviour was observed in case of IDFOSG. The decrease in Cr(VI) uptake degree was found to be ~10% at 1440 min, indicating the stronger interaction of Cr(VI) on surface of IDFOSG and no considerable occurrence of desorption. Secondly, in case of IDTPASG, a steady decrease in Cr(VI) uptake was observed and at the end of the experiment (46% from the original amount), suggesting that this adsorbent is less stable than IDFOSG and some leaching occurred. Considering the results, a contact (shaking) time of 5 min was selected for further experiments.

Optimal sample volume for Cr(VI) uptake was determined by varying the sample volume over a range of 1–10 mL of 1 mg L^{-1} solutions at the already optimized conditions. From Fig. 4 d, samples of either 3 or 5 mL under 100 mg of SGC have higher uptake degree of Cr(VI), without significant differences. Further increase in sample volume showed a slight trend of decreased Cr(VI) uptake degree, reflecting possibly the need of a longer contact time for bigger samples. The 5 mL-size aliquot was chosen for further experiments.
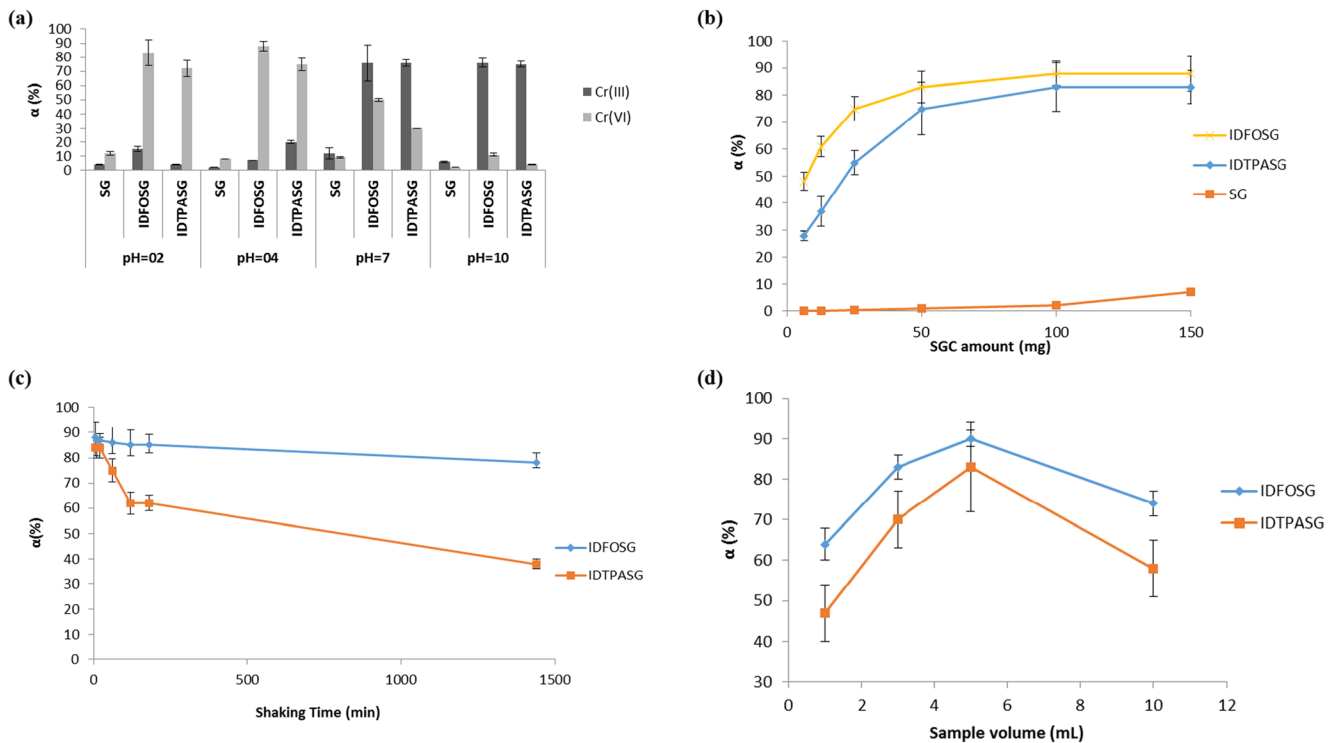
Fig. 4 Sorption optimization experiments. **a** Effect of pH on uptake degree of Cr(III) and Cr(VI) by SGC. **b** Effect of mass on the uptake (α%) of Cr(VI) by IDFOSG, IDTPASG and SG at pH = 4 ($n = 3$). **c** Effect of contact time on the uptake (α%) of Cr(VI) (3 mL; 1 mg L^{-1}; pH 4) by

100 mg of SGC ($n = 3$). **d** Effect of sample volume on the uptake (α%) of Cr(VI) (1 mg L^{-1}; pH 4) by 100 mg of SGC with shaking time of 5 min ($n = 3$)

Effect of potentially interfering ions

The interferences of ions such as Na(I), Mn(II), Cu(II), Zn(II), Ba(II), Al(III) and Fe(III) individually and in a multielemental solution were examined in 5 mL samples containing 1 mg L^{-1} Cr(VI) (Table 1). Cr(VI) uptake degree was not influenced by Na(I) even at a × 4000 excess over Cr(VI). However, competition was important for divalent ions, and attained a maximum of 13% decrease by trivalent ions and multielemental solution. This is due to two factors. Firstly, the trivalent metal ions (which are harder acids) form much stronger complexes with the hard bases DFO and DTPA than do

the divalent metal ions, indicating the significantly more ionic character of the bonds (Kiss & Farkas 1998). In any case, recovery greater than 75% was obtained in every situation, even in multielemental solution. These findings demonstrate that there is a moderate tolerance level towards these ions, and SGC can best serve for Cr removal in an elevated electrolytic environment under optimized conditions.

Sorption isotherms

The sorption data for SGC were fitted using the Langmuir monolayer adsorption model (Fig. 5). Cr(VI) uptake degree

Table 1 Effect of interfering ions on Cr(VI) (1 mgL^{-1}; pH 4) uptake degree (α%) by IDFOSG and IDTPASG (100 mg)

Interfering ions (X)	Ratio X*/Cr(VI)	α% Cr(VI), IDFOSG	α% Cr(VI), IDTPASG
Al^{3+}	4	77.50 ± 1.24	77.94 ± 5.46
Fe^{3+}	6	74.91 ± 5.24	78.59 ± 3.69
Zn^{2+}	100	82.01 ± 1.64	80.56 ± 2.86
Na$^+$	4000	87.75 ± 4.39	84.07 ± 7.14
Mn^{2+}	2	85.38 ± 10.67	83.66 ± 1.06
Ba^{2+}	14	85.64 ± 7.71	83.00 ± 9.13
Cu^{2+}	40	86.07 ± 5.16	82.50 ± 1.40
Multielemental solution	–	75.07 ± 5.16	74.87 ± 3.57

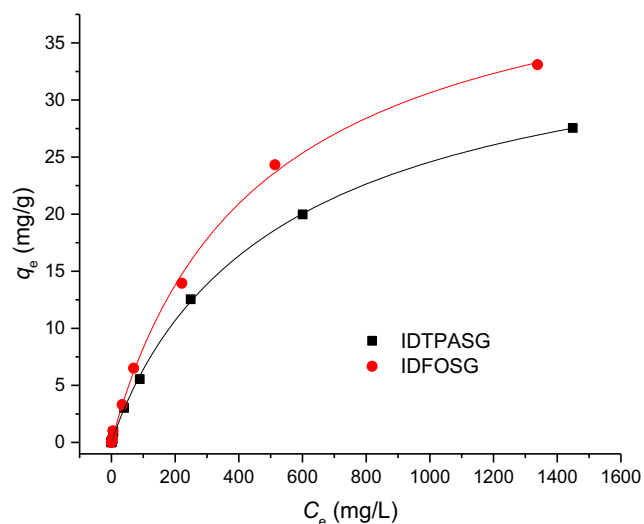*Set at the upper limit allowed by Ordinance 2914/2011 of the Brazilian Ministry of Health

Fig. 5 Langmuir adsorption isotherms for hexavalent chromium onto IDFOSG or IDTPASG (100 mg) at pH 4

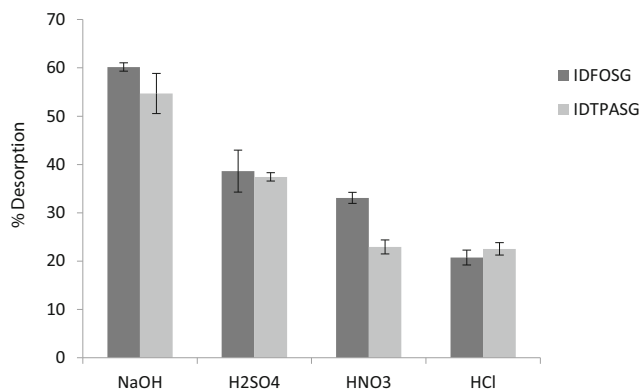**Fig. 6** Desorption studies of 100 mg IDFOSG and IDTPASG preloaded with 1 mgL^{-1} Cr(VI) and equilibrated with 0.1 M solutions of NaOH, H_2SO_4, HNO_3 or HCl

range was 0.5–2000 mg L^{-1}, and metal concentration in the supernatants was calculated from a calibration curve of Cr(VI) ($y = 0.0926\ x - 0.0015$; $R^2 = 0.9992$). The LOD and LOQ of the method calculated by FAAS were 0.01 mg L^{-1} and 0.05 mg L^{-1}, respectively. In the Langmuir equation (Eq. 3):

$$q_e = \frac{q_{max} \times K_L}{1 + (K_L \times C_e)} \tag{3}$$

C_e, q_e and q_{max} are equilibrium concentration (mg L^{-1}), adsorption at equilibrium (mg g^{-1}) and maximum adsorption, respectively (Foo & Hameed 2010). K_L is the adsorption equilibrium constant which serves as an indication of the relative strength of the adsorption process. The isotherm constants are presented in Table 2. A simple monolayer cover of SGC assisted by the presence of chelators describes satisfactorily the Cr(VI) adsorption behaviour, without significant differences in the affinities and an increase of capacity in the case of IDFOSG.

Our materials compare favourably with other low surface area materials such as agricultural residues ($q_{max} \sim$ 0.6 mg g^{-1}) and are on par with some nanomaterials ($q_{max} \sim 15$ mg g^{-1}). In contrast, synthetic polymers have displayed $q_{max} > 100$ mg g^{-1} for chromium species (Pakade et al. 2019).

Stability and regeneration

To evaluate stability and regeneration of SGC, desorption experiments were performed. It is observed from Fig. 6 that maximum Cr(VI) desorption for IDFOSG or IDTPASG happened with 0.1 M NaOH solution. This is probably due to the changes in charge and concentration of Cr(VI) species as discussed above, resulting in the electrostatic repulsion as well as decreasing levels of $HCrO_4^-$ for sorption. This can also be due to interference of OH^- ions competing with chromate. The net result is the weakening of the interaction of Cr(VI) due to unavailability of active sites for interaction as previously discussed (Bhatt et al. 2015).

Three repetitive cycles of sorption-desorption were carried out to measure the capacity of regeneration and stability of both IDFOSG and IDTPASG, and a decrease in percent uptake of Cr(VI) of ∼ 17% and 35% was observed for IDFOSG and IDTPASG respectively (Fig. 7). It is obvious from the results that the binding performance of IDFOSG was less affected when compared to IDTPASG after successive cycles; hence, IDFOSG is better suited to remove Cr(VI) from aqueous solutions.
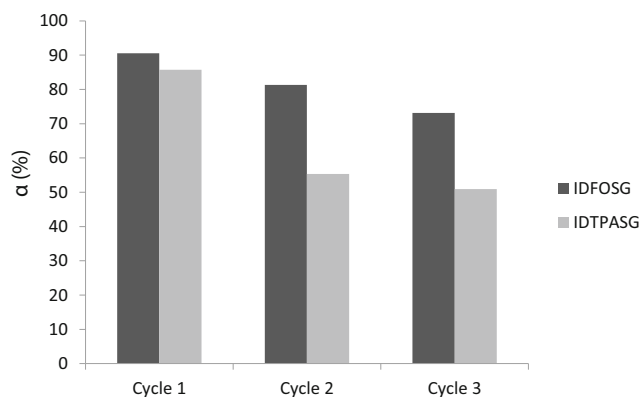

Fig. 7 Effect of sorption-desorption repetitive cycles on the uptake degree of Cr(VI) by 100 mg IDFOSG and IDTPASG preloaded with 1 mgL^{-1} Cr(VI)

Table 2 Isotherm constants for IDFOSG and IDTPASG adsorption

	IDFOSG	IDTPASG
q_{max} (mg/g)	45.3 ± 2.8	38.6 ± 1.3
K_L (10^{-3} L/mg)	2.58 ± 0.62	2.55 ± 0.30
R^2	0.9985	0.9996

Conclusion

The surface-grafted siderophore deferrioxamine (DFO) on silica gel had a generally better performance than its DTPA counterpart as a chromium adsorbent. SGC in general and IDFOSG in particular are promising sorption materials for the remediation of chromium pollution.

References

Aaseth J, Skaug MA, Cao Y, Andersen O (2015) Chelation in metal intoxication—principles and paradigms. J Trace Elem Med Biol 31:260–266

Alberti G, Emma G, Colleoni R, Pesavento M, Nurchi VM, Biesuz R (2014) Novel DFO-functionalized mesoporous silica for iron sensing. Part 2. Experimental detection of free iron concentration (pFe) in urine samples. Analyst 139:3940–3948

Alberti G, Quattrini F, Colleoni R, Nurchi VM, Biesuz R (2015) Deferoxamine–paper for iron (III) and vanadium (V) sensing. Chem Pap 69:1024–1032

Alta ECP, Goswami D, Machini MT, Silvestre DM, Nomura CS, Espósito BP (2014) Desferrioxamine-caffeine (DFCAF) as a cell permeant moderator of the oxidative stress caused by iron overload. BioMetals 27:1351–1360

Baccan MM, Chiarelli-Neto O, Pereira RMS, Espósito BP (2012) Quercetin as a shuttle for labile iron. J Inorg Biochem 107:34–39

Beppu M, Vieira R, Aimoli C, Santana C (2007) Crosslinking of chitosan membranes using glutaraldehyde: effect on ion permeability and water absorption. J Membr Sci 301:126–130

Bertoluzza A, Fagnano C, Morelli MA, Gottardi V, Guglielmi M (1982) Raman and infrared spectra on silica gel evolving toward glass. J Non-Cryst Solids 48:117–128

Bhatt R, Sreedhar B, Padmaja P (2015) Adsorption of chromium from aqueous solutions using crosslinked chitosan–diethylenetriaminepentaacetic acid. Int J Biol Macromol 74:458–466

Brazil Mnistry of Health, 914/2011 (2011): procedures for control and surveillance of water quality for human consumption and its potability standards, (Published in Official Gazette, 2011).

Carvalho AA, Silvestre DM, Leme FO, Naozuka J, Intima DP, Nomura CS (2019) Feasibility of measuring Cr (III) and Cr (VI) in water by laser-induced breakdown spectroscopy using ceramics as the solid support. Microchem J 144:33–38

Christoffersen M, Thyregod H, Christoffersen J (1987) Effects of aluminum (III), chromium (III), and iron (III) on the rate of dissolution of calcium hydroxyapatite crystals in the absence and presence of the chelating agent desferrioxamine. Calcif Tissue Int 41:27–30

Currie LA (1995) Nomenclature in evaluation of analytical methods including detection and quantification capabilities (IUPAC recommendations 1995). Pure Appl Chem 67:1699–1723

Darr D, Zarilla KA, Fridovich I (1987) A mimic of superoxide dismutase activity based upon desferrioxamine B and manganese (IV). Arch Biochem Biophys 258:351–355

Dey R, Jha U, Singh A, Samal S, Ray AR (2006) Extraction of metal ions using chemically modified silica gel covalently bonded with 4, 4′-diaminodiphenylether and 4, 4′-diaminodiphenylsulfone-salicylaldehyde Schiff bases. Anal Sci 22:1105–1110

Domingo JL (2006) Aluminum and other metals in Alzheimer's disease: a review of potential therapy with chelating agents. J Alzheimers Dis 10:331–341

Dong H, Deng J, Xie Y, Zhang C, Jiang Z, Cheng Y, Hou K, Zeng G (2017) Stabilization of nanoscale zero-valent iron (nZVI) with modified biochar for Cr (VI) removal from aqueous solution. J Hazard Mater 332:79–86

Duckworth OW, Sposito G (2005) Siderophore− manganese (III) interactions. I Air-Oxidation of Manganese (II) Promoted by Desferrioxamine B. Environ Sci Technol 39:6037–6044

Dutton J, Fisher NS (2011) Bioaccumulation of as, cd, Cr, hg (II), and MeHg in killifish (Fundulus heteroclitus) from amphipod and worm prey. Sci Total Environ 409:3438–3447

Foo KY, Hameed BH (2010) Insights into the modeling of adsorption isotherm systems. Chem Eng J 156:2–10

Gabizon A, Hliberty J, Straubinger RM, Price DC, Papahadjopoulos D (1988) An improved method for in vivo tracing and imaging of liposomes using a gallium 67-deferoxamine complex. J Liposome Res 1:123–135

Hughes MA, Rosenberg E (2007) Characterization and applications of poly-acetate modified silica polyamine composites. Sep Sci Technol 42:261–283

Jal P, Dutta R, Sudarshan M, Saha A, Bhattacharyya S, Chintalapudi S, Mishra BK (2001) Extraction of metal ions using chemically modified silica gel: a PIXE analysis. Talanta 55:233–240

Jitianu A, Crisan M, Meghea A, Rau I, Zaharescu M (2002) Influence of the silica based matrix on the formation of iron oxide nanoparticles in the Fe 2 O 3–SiO 2 system, obtained by sol–gel method. J Mater Chem 12:1401–1407

Kandile NG, Nasr AS (2014) New hydrogels based on modified chitosan as metal biosorbent agents. Int J Biol Macromol 64:328–333

Karthik C, Ramkumar VS, Pugazhendhi A, Gopalakrishnan K, Arulselvi PI (2017) Biosorption and biotransformation of Cr (VI) by novel Cellulosimicrobium funkei strain AR6. J Taiwan Inst Chem Eng 70: 282–290

Ke Jian Liu XS, Dalal NS (1997) Synthesis of Cr(IV)-GSH, its identification and its free hydroxyl radical generation: a model compound for Cr(VI) carcinogenicity. Biochem Biophys Res Commun 235: 54–58

Kiss T, Farkas E (1998) Metal-binding ability of desferrioxamine B. J Incl Phenom Mol Recognit Chem 32:385–403

Kotaś J, Stasicka Z (2000) Chromium occurrence in the environment and methods of its speciation. Environ Pollut 107:263–283

Kumar ASK, Rajesh N (2013) Exploring the interesting interaction between graphene oxide, Aliquat-336 (a room temperature ionic liquid) and chromium (VI) for wastewater treatment. RSC Adv 3: 2697–2709

Li J, Miao X, Hao Y, Zhao J, Sun X, Wang L (2008) Synthesis, aminofunctionalization of mesoporous silica and its adsorption of Cr (VI). J Colloid Interface Sci 318:309–314

Li Z, Li T, An L, Fu P, Gao C, Zhang Z (2016) Highly efficient chromium (VI) adsorption with nanofibrous filter paper prepared through electrospinning chitosan/polymethylmethacrylate composite. Carbohydr Polym 137:119–126

Liang P, Chen X (2005) Preconcentration of rare earth elements on silica gel loaded with 1-phenyl-3-methyl-4-benzoylpyrazol-5-one prior to their determination by ICP-AES. Anal Sci 21:1185–1188

Ljunggren L, Altrell I, Risinger L, Johansson G (1992) Trace enrichment of aluminium ions on immobilized desferrioxamine. Anal Chim Acta 256:75–80

Lyu H, Tang J, Huang Y, Gai L, Zeng EY, Liber K, Gong Y (2017) Removal of hexavalent chromium from aqueous solutions by a

novel biochar supported nanoscale iron sulfide composite. Chem Eng J 322:516–524

Maria Chong A, Zhao X (2003) Functionalization of SBA-15 with APTES and characterization of functionalized materials. J Phys Chem B 107:12650–12657

Michael Sperling SXABW (1992) Determination of chromium(III) and chromium(VI) in water using flow injection on-line Preconcentration with selective adsorption on activated alumina and flame atomic absorption spectrometric detection. Anal Chem 3101-3108

Miretzky P, Cirelli AF (2010) Cr (VI) and Cr (III) removal from aqueous solution by raw and modified lignocellulosic materials: a review. J Hazard Mater 180:1–19

Najafi M, Yousefi Y, Rafati A (2012) Synthesis, characterization and adsorption studies of several heavy metal ions on amino-functionalized silica nano hollow sphere and silica gel. Sep Purif Technol 85:193–205

Oves M, Khan MS, Zaidi A (2013) Biosorption of heavy metals by bacillus thuringiensis strain OSM29 originating from industrial effluent contaminated north Indian soil. Saudi J Biologic Sci 20:121–129

Pakade VE, Tavengwa NT, Madikizela LM (2019) Recent advances in hexavalent chromium removal from aqueous solutions by adsorptive methods. RSC Adv 9:26142–26164

Parker HG, Low-Beer ADG, Isaac EL (1962) Comparison of retention and organ distribution of Am241 and Cf252 in mice: the effect of in vivo DTPA chelation. Health Phys 8:679–684

Powell P, Cline G, Reid C, Szaniszlo P (1980) Occurrence of hydroxamate siderophore iron chelators in soils. Nature 287:833

Qiu J, Wang Z, Li H, Xu L, Peng J, Zhai M, Yang C, Li J, Wei G (2009) Adsorption of Cr (VI) using silica-based adsorbent prepared by radiation-induced grafting. J Hazard Mater 166:270–276

Rai D, Sass BM, Moore DA (1987) Chromium (III) hydrolysis constants and solubility of chromium (III) hydroxide. Inorg Chem 26:345–349

Randal J, Keller JDR, Grover TA (1991) Spectrophotometric and ESR evidence for vanadium(IV) deferoxamine complexes. J Inorg Biochem 41:269–276

Repo E, Kurniawan TA, Warchol JK, Sillanpää ME (2009) Removal of co (II) and Ni (II) ions from contaminated water using silica gel functionalized with EDTA and/or DTPA as chelating agents. J Hazard Mater 171:1071–1080

Repo E, Malinen L, Koivula R, Harjula R, Sillanpää M (2011) Capture of co (II) from its aqueous EDTA-chelate by DTPA-modified silica gel and chitosan. J Hazard Mater 187:122–132

Sari A, Mendil D, Tuzen M, Soylak M (2008) Biosorption of cd (II) and Cr (III) from aqueous solution by moss (Hylocomium splendens) biomass: equilibrium, kinetic and thermodynamic studies. Chem Eng J 144:1–9

Schwabe R, Anke MK, Szymańska K, Wiche O, Tischler D (2018) Analysis of desferrioxamine-like siderophores and their capability to selectively bind metals and metalloids: development of a robust analytical RP-HPLC method. Res Microbiol 169:598–607

Sethy TR, Sahoo PK (2019) Highly toxic Cr (VI) adsorption by (chitosan-g-PMMA)/silica bionanocomposite prepared via emulsifier-free emulsion polymerisation. Int J Biol Macromol 122:1184–1190

Shriner RL, Fuson R, Curtin DY (1948) Thesystematic identification of organic compounds. John Wiley and Sons, New York, pp 202–207

Siebner-Freibach H, Yariv S, Lapides Y, Hadar Y, Chen Y (2005) Thermo-FTIR spectroscopic study of the siderophore ferrioxamine B: spectral analysis and stereochemical implications of iron chelation, pH, and temperature. J Agric Food Chem 53:3434–3443

Slobodien MJ, Brodsky A, Ke CH, Horm I (1973) Removal of zinc from humans by DTPA chelation therapy. Health Phys 24:327–330

Su B-L, Moniotte N, Nivarlet N, Chen L-H, Fu Z-Y, Desmet J, Li J (2011) Fl–DFO molecules@ mesoporous silica materials: highly sensitive and selective nanosensor for dosing with iron ions. J Colloid Interface Sci 358:136–145

Sugumaran D, Karim KJA (2017): Removal of copper (II) ion using chitosan-graft-poly (methyl methacrylate) as adsorbent. eProceedings chemistry 2

Takagai Y, Takahashi A, Yamaguchi H, Kubota T, Igarashi S (2007) Adsorption behaviors of high-valence metal ions on desferrioxamine B immobilization nylon 6, 6 chelate fiber under highly acidic conditions. J Colloid Interface Sci 313:359–362

Takahashi C, Turner A, Millward G, Glegg G (2012) Persistence and metallic composition of paint particles in sediments from a tidal inlet. Mar Pollut Bull 64:133–137

Tülü M, Geckeler KE (1999) Synthesis and properties of hydrophilic polymers. Part 7. Preparation, characterization and metal complexation of carboxy-functional polyesters based on poly(ethylene glycol). Polym Int 48:909–914

Umemura M, Kim J-H, Aoyama H, Hoshino Y, Fukumura H, Nakakaji R, Sato I, Ohtake M, Akimoto T, Narikawa M, Tanaka R, Fujita T, Yokoyama U, Taguri M, Okumura S, Sato M, Eguchi H, Ishikawa Y (2017) The iron chelating agent, deferoxamine detoxifies Fe(Salen)-induced cytotoxicity. J Pharmacol Sci 134:203–210

Wani P, Sunday O, Kehinde A, Oluwaseyi L, Wasiu I, Wahid S (2018) Antioxidants and chromium reductases by Penibacillus species enhance the growth of soybean under chromium stress. Int J Environ Sci Technol 15:1531–1542

Wenk J, Sabiwalsky A, Dissemond J, Meewes C, Brenneisen P, Wlaschek M, Scharffetter-Kochanek K, Foitzik A, Achterberg V, Reitz A (2001) Selective pick-up of increased iron by deferoxamine-coupled cellulose abrogates the iron-driven induction of matrix-degrading metalloproteinase 1 and lipid peroxidation in human dermal fibroblasts in vitro: a new dressing concept. J Investig Dermatol 116:833–839

White L, Tripp C (2000) Reaction of (3-aminopropyl) dimethylethoxysilane with amine catalysts on silica surfaces. J Colloid Interface Sci 232:400–407

Wu P, Chen H, Cheng G, Hou X (2009) Exploring surface chemistry of nano-TiO 2 for automated speciation analysis of Cr (iii) and Cr (vi) in drinking water using flow injection and ET-AAS detection. J Anal At Spectrom 24:1098–1104

Xianglin Shi XS, Peter M. Gannett, and N. S. Dalal (1992): Deferoxamine inhibition of Cr(V)-mediated radicaI generation and deoxyguanine hydroxylation: ESR and HPLC evidence ARCHIVES OF BIOCHEMISTRY AND BIOPHYSICS 293, 281–286

Yang J-K, Lee S-M (2006) Removal of Cr (VI) and humic acid by using TiO2 photocatalysis. Chemosphere 63:1677–1684